Polar Geosci., **19**, 37–61, 2006

Calc-silicate rocks and marbles from Lützow-Holm Complex, East Antarctica, with special reference to the mineralogy and geochemical characteristics of calc-silicate mega-boudins from Rundvågshetta

M. Satish-Kumar[1*], Yoichi Motoyoshi[2], Yoshimitsu Suda[2], Yoshikuni Hiroi[3] and Shin-ichi Kagashima[4]

[1]*Institute of Geosciences, Shizuoka University, Oya 836, Suruga-ku, Shizuoka, 422-8529*
[2]*National Institute of Polar Research, Kaga 1-come, Itabashi-ku, Tokyo 173-8515*
[3]*Department of Earth Sciences, Chiba University, Yayoi-cho 1–33, Inage-ku, Chiba 263-8522*
[4]*Department of Earth and Environmental Sciences, Faculty of Science, Yamagata University, Kojirakawa-machi 1–4–12, Yamagata 990-8560*
[*]*Corresponding author. E-mail: smsatis@ipc.shizuoka.ac.jp*

(Received April 6, 2006; Accepted July 6, 2006)

Abstract: We report here the mode of occurrence of calc-silicate rocks and marbles from the Lützow-Holm Complex, East Antarctica, and a worked example from Rundvågshetta. Calc-silicate boudins were observed in Cape Hinode, Akarui Point, Byôbu Rock, Skarvsnes, Skallevikshalsen and Rundvågshetta, whereas they were reported earlier from Sinnan Rock, Cape Ryûgû, Akebono Rock, Cape Hinode, Niban Rock, Kasumi Rock, Daruma Rock, Cape Omega, Langhovde, Ytrehovdeholmen and Skarvsnes. They vary in size from decimeters to few meters and are commonly enclosed within pelitic or psammitic gneisses. In addition, extensive layers of marbles and calc-silicate rocks are distributed in Skallevikshalsen. The calc-silicate mega-boudins within the layered pyroxene-gneiss from Rundvågshetta, up to 5 m long and 2 m thick, comprises of coarse to medium grained assemblage of scapolite + anorthite + garnet + clinopyroxene + calcite + quartz + titanite ± wollastonite. Co-existing scapolite and plagioclase suggest a "*minimum*" estimate of peak metamorphic temperature of ~830℃. Peak metamorphic mineral assemblages equilibrated at moderate to high X_{CO2} conditions (0.3–0.7) and temperatures between 850 and 1000℃, consistent with the ultrahigh temperature metamorphic conditions reported in the region. Multistage garnet corona formation preserved in the calc-silicate assemblage suggests a local increase in hydrous fluid activity during retrogression. Preliminary bulk rock geochemistry of different mineralogical zones in the boudin shows chemical potential gradients in some major elements, especially SiO_2, Al_2O_3 and CaO, possibly controlled by the compositional variations in the protolith. Altogether, these results suggest that calc-silicate rocks preserve information on the metamorphic evolution and help us in deducing the geodynamic evolution of high-grade terrains.

key words: calc-silicate boudins, Lützow-Holm Complex, fluid-rock interaction, *P-T*-fluid history, garnet corona textures

1. Introduction

During the past couple of decades, calc-silicate rocks and marbles in the high-grade metamorphic terrains have gained a great deal of attention among petrologists (*e.g.* Valley and Essene, 1980; Hiroi *et al*., 1987; Warren *et al*., 1987; Motoyoshi *et al*., 1991; Harley and Buick, 1992; Klemd *et al*., 1994; Buick *et al*., 1994; Fitzsimons and Harley, 1995; Satish-Kumar and Harley, 1998; Piazolo and Markl, 1999; Satish-Kumar *et al*., 2001; Sengupta and Raith, 2002; Dasgupta and Pal, 2005). Although voluminously minor in occurrence, the key factors that endorse the usefulness of calc-silicate rocks and marbles in deducing the crustal evolution include; 1) widespread occurrence as thin layers and boudins enclosed within the metasedimentary sequences (*e.g.* Hiroi *et al*., 1987; Harley *et al*., 1994); 2) preservation of characteristic mineral assemblages representing the peak metamorphic conditions (*e.g.* Harley and Buick, 1992); 3) preservation of reaction textures in response to changes in the *P-T*-fluid history (*e.g.* Harley and Buick, 1992; Satish-Kumar and Harley, 1998); 4) response of mineral chemistry with changes in oxygen fugacity conditions (*e.g.* Dasgupta and Pal, 2005); and 5) resistance to partial melting. Several recent studies have also emphasized the extreme efficacy of geochemical characteristics of calc-silicate rocks, especially the carbon and oxygen stable isotopes, in deducing the fluid-rock history (Cartwright and Valley, 1991; Ferry, 1992; Ferry *et al*., 1998; Buick *et al*.,1994, 1997; Tsuchiya *et al*., 1992; Satish-Kumar and Wada, 1997; Satish-Kumar *et al*., 1998). Furthermore, calc-silicate rocks and marbles are geochemically distinct from the associated metasedimentary rocks thus forming ideal rock units for understanding the mobility of elements and metasomatism in the lower crust (*e.g.* Buick *et al*., 1993; Ferry, 1992). Thus, calc-silicate rocks are considered to be ideal petrologic and geochemical markers for understanding the evolution of the lower to middle continental crust.

As is the case with many high-grade terrains worldwide, calc-silicate rocks and marbles occur sporadically in the Pan-African high-grade metamorphic terrain exposed in the Lützow-Holm Bay region, East Antarctica. Hiroi *et al.* (1987) described the salient mineralogy and petrologic significance of calc-silicate rocks and delineated two important mineral isograds, which helped in assigning a progressive metamorphism in the Lützow-Holm Complex (LHC). Considering the importance of calc-silicate rocks, we identified several new occurrences during the JARE-46 geologic expedition within the LHC. In this contribution, we describe the mode of occurrence of calc-silicate rocks and marbles from several outcrops in the Prince Olav Coast and Sôya Coast in the Lützow-Holm Bay region. We further focus on the calc-silicate mega-boudins from Rundvågshetta, the locality where the highest peak metamorphic *P-T* conditions were reported in this complex. Based on the general mineralogy, mineral chemistry and bulk rock chemical features of the Rundvågshetta calc-silicate mega-boudins, we discuss the *P-T*-fluid history and the significance of calc-silicate rocks in unraveling the metamorphic-fluid evolution of the region.

2. Geology of Lützow-Holm Complex

The eastern Dronning Maud Land in East Antarctica comprises of Archaean to

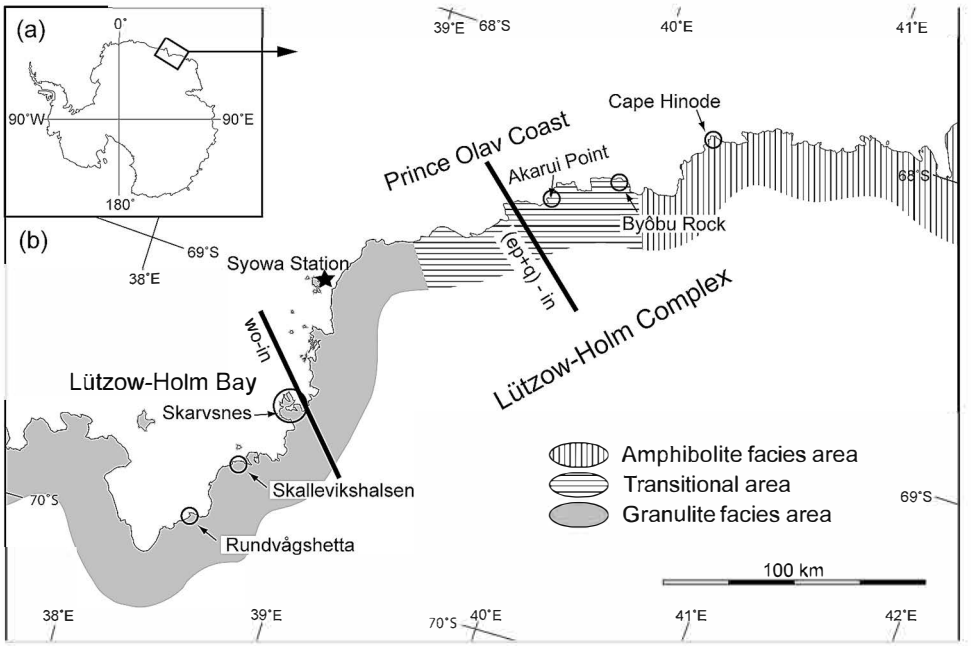

Fig. 1. Schematic map of Lützow-Holm Complex showing the progressive increase in metamorphic grade from East to West as evidenced by the presence of index minerals in various lithologies. Two calc-silicate isograds are also shown (after Hiroi et al., 1987). Sampling localities of calc-silicate rocks and marbles during JARE-46 geological field expedition are shown.

Early Proterozoic Napier Complex, Proterozoic Rayner Complex, Late Proterozoic to Early Paleozoic Lützow-Holm Complex and Yamato Belgica Complex, from east to west. Within these terrains, the Lützow-Holm Complex (LHC) forms an important segment of predominantly metasedimentary rock units that are considered to have deposited as marginal sea sediments in the basin that separated East and West Gondwana. Several earlier studies have reviewed the geology of this unique metamorphic complex, which exposes a continuous oblique deep crustal section with a metamorphic gradient from east to west (Hiroi *et al*., 1983, 1986, 1987, 1991; Shiraishi *et al*., 1994, 2003). Progressive metamorphism has been accredited to the Lützow-Holm Complex (Fig. 1), with an increase in metamorphic grade from amphibolite facies in the northeast to granulite facies in the southwest region, with a clockwise *P-T* evolution and a thermal maximum at Rundvågshetta (Hiroi *et al*., 1987; Motoyoshi *et al*., 1989; Motoyoshi and Ishikawa, 1997). Geochronologic studies indicate that this terrain was tectonothermally active during the Cambrian orogeny (Shiraishi *et al*., 1994, 2003), in the waning stages of Pan-African tectonothermal event, in analogy with many terrains of adjoining East Gondwana continental fragments.

3. Previous studies

Although calc-silicate rocks, marbles and skarn occur widespread in LHC there are less number of comprehensive studies on their petrologic aspects. Earliest reports on marbles and skarn occurrences are from Skallevikshalsen (Matsueda *et al.,* 1983). Hiroi *et al.* (1987) carried out a detailed study on the occurrence, mineralogy and reaction textures observed in the calc-silicate rocks and marbles in the Prince Olav Coast and Sôya Coast and recognized wollastonite-in and epidote-out isograds (Fig. 1). In a companion study, Hiroi and Kojima (1988) reported the mode of occurrence and mineralogical characteristics of dolomitic marbles from Kasumi Rock in the Prince Olav Coast.

Tsuchiya *et al.* (1992) quantified the fluid-rock interaction between thin layers of marbles and pelitic layers at Sør Rondane Mountains, applying carbon and oxygen stable isotope variation across marble layers. Applying the state of the art microscale stable isotope studies within single crystals of calcite in marbles from Skallen region, Satish-Kumar and Wada (1997) and Satish-Kumar *et al.* (1998) identified evidence for the movement of water-rich fluids through selected grain boundaries in marbles. Furthermore, recent results indicate strontium isotope anomalies that suggest complete recrystallization and isotopic resetting with hyper-saline fluids that evolved from the adjacent metapelitic rocks during prograde or peak metamorphism (Satish-Kumar *et al*., 2003). Carbon stable isotope thermometry was applied to the graphite-bearing marbles from Skallen, which yielded possible peak metamorphic temperature estimates of around 860°C (Satish-Kumar and Wada, 2000).

Occurrence of scapolite boudins in the Skallen region were the focus of recent studies, which identified large compositional variations in single scapolite grains corresponding to the changing fluid conditions in the lower to middle crust. Kusachi *et al.* (1999) investigated the zoning patterns observed in scapolite from Skallen region. Satish-Kumar *et al.* (2005) identified fractures within scapolite poikiloblasts through which carbonic fluid percolated and altered the Cl-rich scapolite to carbonate-rich scapolite. Further in a detail investigation using major, trace and rare earth element geochemical features and fluid inclusion studies on scapolite grains, Satish-Kumar *et al.* (2006a), deduced the changing fluid-rock interaction history of scapolite. It was concluded that the early formed chlorine-rich scapolite might have an origin related to evaporite protoliths, which were subsequently infiltrated by carbonic fluids, as evidenced by abundant fluid inclusions observed along healed fractures adjacent to which carbonation reactions progressed.

Thus, regardless of some systematic studies on specific calc-silicate rock occurrences, the present status of research on calc-silicate rocks and marbles are far from enough in obtaining the wealth of information preserved in these rocks.

4. Mode of occurrence of calc-silicate boudins in the Lützow Holm Complex

Below, we describe the general mode of occurrence of calc-silicate rocks and marbles in the LHC studied during the JARE-46 expedition. As a case study, we describe in detail the field occurrence, mineralogical features and bulk rock geochemistry of calc-silicate mega-boudins from Rundvågshetta.

4.1. Cape Hinode

In contrast with the well-layered pelitic to psammitic and intermediate lithologies that are common in the LHC, Cape Hinode exposes a monotonous rock unit that closely resemble metamorphosed anorthosite. Preliminary results on petrological aspects (Hiroi *et al*., 2005) and geochronology (Motoyoshi *et al*., 2004) suggest an allocthonous origin for this rock unit that display contrasting tectonothermal history when compared with the other rock units in the LHC. Regardless, we found out several occurrences of calc-silicate boudins that range in size from few centimeters to more than a meter. In the eastern part of Cape Hinode, about one kilometer NW of Maigo Peak, numerous calc-silicate boudins of varying size occur within a few meters thick zone of anorthositic gneiss (Fig. 2a). They are rounded to oval in shape (Fig. 2b). Mineralogically, these calc-silicate boudins are conspicuously rich in garnet in the core of the boudin, while rims comprises of clinopyroxene＋plagioclase with subordinate amounts of epidote.

Another cluster of calc-silicate boudins were observed near the Penguin Heights. Typically, these boudins are elongated lens shaped (Fig. 2c) or irregular (Fig. 2d). Field observations suggest that these boudins are mineralogically zoned with garnet-bearing assemblages in the core and felsic mineral assemblages in the contact with the

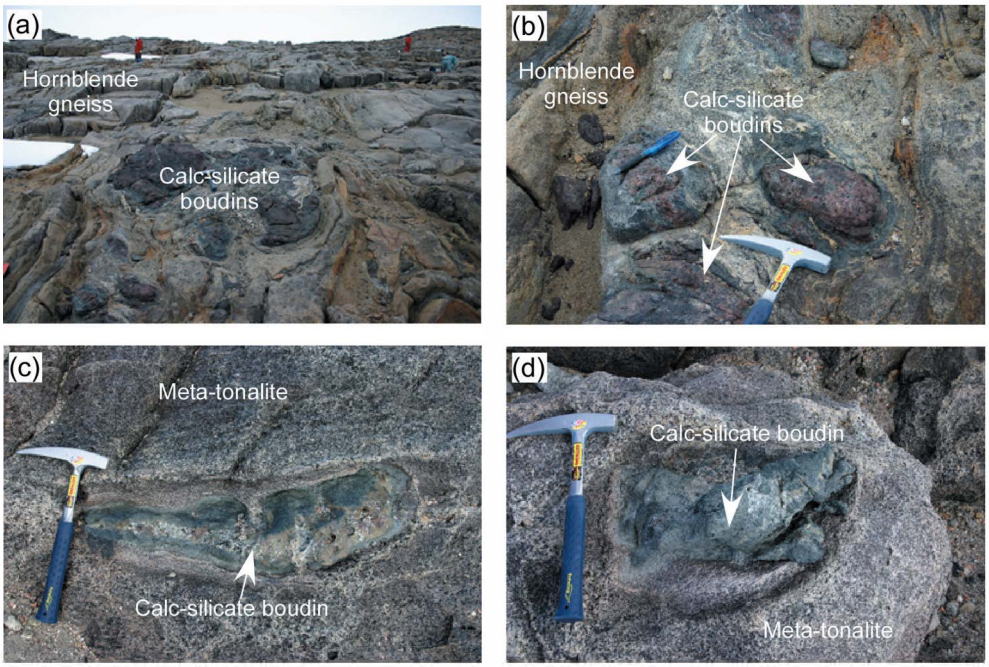

Fig. 2. Field photographs showing the occurrence of calc-silicate boudins at Cape Hinode. (a) A meter wide hornblende gneiss zone within which numerous calc-silicate boudins are observed (68°8.521S; 42°42.877E). (b) Calc-silicate boudins occurring with leucocratic veins traversing between the boudins. Boudins generally show mineralogical zones with garnet-bearing assemblage in the core. (c) Field occurrence of irregular shaped calc-silicate boudin near Penguin Heights at Cape Hinode (68°8.622S; 42°39.614E). (d) Lens shaped calc-silicate boudin at Cape Hinode.

country rocks (Fig. 2c).

4.2. Akarui Point

Akarui Point is situated in the transition zone between the amphibolite-facies area and the granulite-facies area of the LHC (Hiroi *et al*., 1987). This region mainly comprises of biotite-hornblende gneiss and felsic gneiss (Yanai *et al*., 1984). Mappable layers of saphhirine-bearing assemblages and sporadic occurrence of ultramafic blocks are characteristic in this region. The occurrence of pelitic assemblages that characteristically contain kyanite inclusions within garnet and sillimanite in the matrix indicates a clockwise *P-T* path, similar to other regions in the LHC (Hiroi *et al*., 1986). Couple of large scale regional antiforms and a synform, were reported by Yanai *et al.* (1984) that corresponds to at least two stages of deformation. Further, in a recent study, Ikeda and Kawakami (2004) recognized an earlier phase of deformation.

Calc-silicate boudins were identified in two localities in the Akarui Point exposure. Meter scale rounded calc-silicate boudins (Fig. 3a), identified in migmatized gneiss near Itibô Peak, comprises of garnet-epidote-bearing assemblages. Epidote occurs in the core portions as aggregates (Fig. 3b). In the south of Donburi Pond area, lens shaped calc-silicate rocks occur within the layered migmatitic gneiss adjacent to a sillimanite-

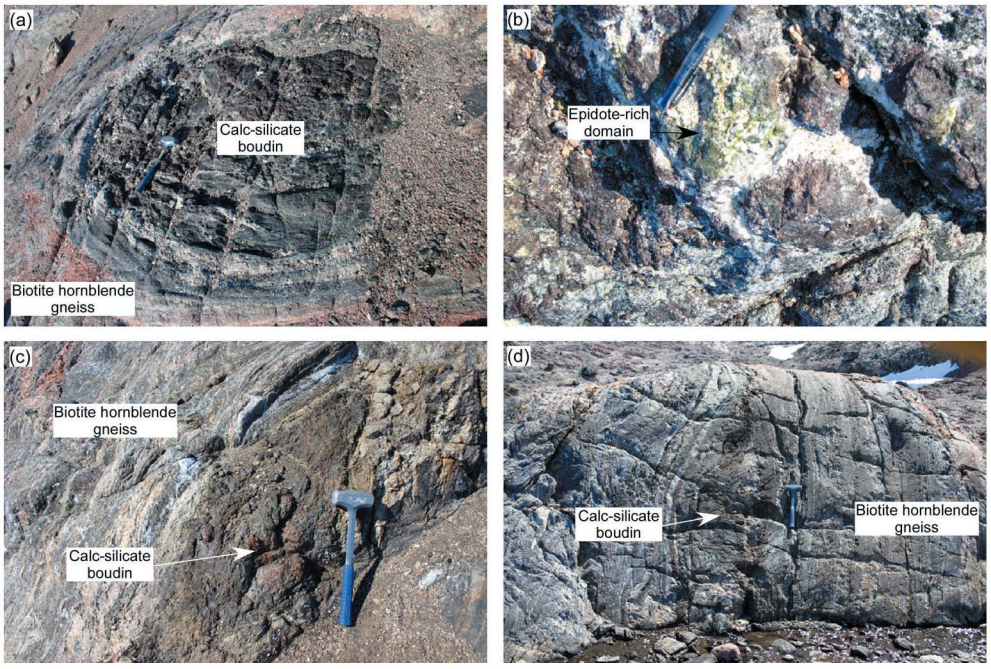

Fig. 3. (a) Field occurrence of meter-scale calc-silicate boudin at Akarui Point (68°29.946S; 41°24.761E). (b) Epidote aggregate within the calc-silicate boudin. (c) Field occurrence of calc-silicate lens within the layered migmatites near Donburi Lake (68°30.239S; 41°24.092E). (d) A lens shaped calc-silicate boudin at Akarui Point. Note the garnet-rich assemblage in the core portion of the boudin.

bearing metapelite horizon (Fig. 3c). Garnet-rich zones were identified in the core portions in these calc-silicate rocks (Fig. 3d).

4.3. Byôbu Rock

The Byôbu Rock exposure comprises of predominantly well-layered garnet-biotite quartzo-feldspathic gneiss, hornblende-biotite gneiss and garnet-sillimanite-graphite gneiss (Satish-Kumar *et al*., 2006b). Thin layers of garnet-leucogranite and amphibolite occur within the pelitic gneiss. Gneissic rock units in this locality are subjected to anatexis to variable extent.

A thin (~10 cm) lens of calc-silicate rock was observed within the amphibolite layer at Byôbu Rock. This lens comprises of clinopyroxene and plagioclase, with subordinate amounts of titanite. Quartz and calcite occur in accessory amounts.

4.4. Skarvsnes

Skarvsnes, situated about 40 km south of Syowa Station, is the largest ice-free outcrop in the LHC. This region is characterized by mostly gneissose rocks. According to Ishikawa, T. *et al.* (1977), pyroxene gneiss, garnet-biotite gneiss and hornblende gneiss form the major lithologic units here, with subordinate amounts of basic rocks, migmatites, granitic rocks and pegmatites. Several generations of fold structures (at least 3, Ishikawa, T. 1976), fractures and thrusts were identified in this region. Hiroi *et al.* (1987) described the occurrence of calc-silicate boundins in this outcrop.

Scores of decimeter scale calc-silicate boudins are distributed in Skarvsnes. The calc-silicate boudins are found within the garnet-biotite gneisses. Typically, they are rounded or oval in shape. Maximum size reaches up to 50 cm. Mineral assemblages vary between different boudins (Fig. 4). Some boudins are calcite-free, completely converted into calc-silicate minerals, with concentric mineralogical zoning: Grossular＋wollastonite＋scapolite＋clinopyroxene-bearing assemblage in the core zone, grossular ＋scapolite＋clinopyroxene in the mantle zone, scapolite＋clinopyroxene＋calcite＋quartz in the inner rim and anorthite＋quartz＋clinopyroxene in the outer rim. Some of them retain calcite in the core, whereas some have graphite in the rim portions. A

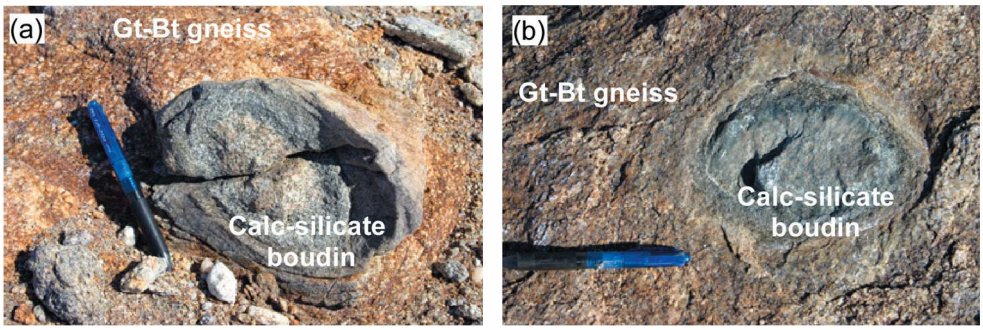

Fig. 4. Field occurrences of calc-silicate boudins in Skarvsnes. (a) A typical rounded calc-silicate boudin within the garnet-biotite gneiss (69°27.377S; 39°35.724E). (b) Mineralogically zoned rounded calc-silicate boudin showing garnet-bearing assemblage in the core.

detailed petrologic study of these calc-silicate boudins will be reported elsewhere.

4.5. Skallevikshalsen

Skallevikshalsen is situated about 70 km southwest of Syowa Station. This region is dominated by orthogneiss, paragneiss, marbles and skarn (Yoshida, 1977). These rock units can be further classified into orthopyroxene felsic gneiss, garnet-sillimanite gneiss, garnet-biotite gneiss and marbles, with subordinate amounts of garnet-spinel-sillimanite gneiss and mafic gneiss. In a recent study, peak metamorphic pressure-temperature condition of this region was estimated to be between 6 and 12 kbar and 770 and 960°C, respectively (Yoshimura *et al.*, 2004). Spinel+quartz assemblage was reported by Kawakami and Motoyoshi (2004) in the outermost core of garnet in garnet-sillimanite leucogneiss substantiating the earlier reports on high-temperature peak metamorphism at Skallevikshalsen.

Marble layers and skarns are common in Skallevikshalsen. Marble layers occur conformably with thickness up to several tens of meters (Fig. 5a). Several typical high-grade marble mineral assemblages are observed, which include dolomitic and calcitic marbles (graphite-bearing) with a variety of silicate mineral assemblages comprising of humite-forsterite-spinel-phlogopite-amphiboles. Various kinds of skarn oc-

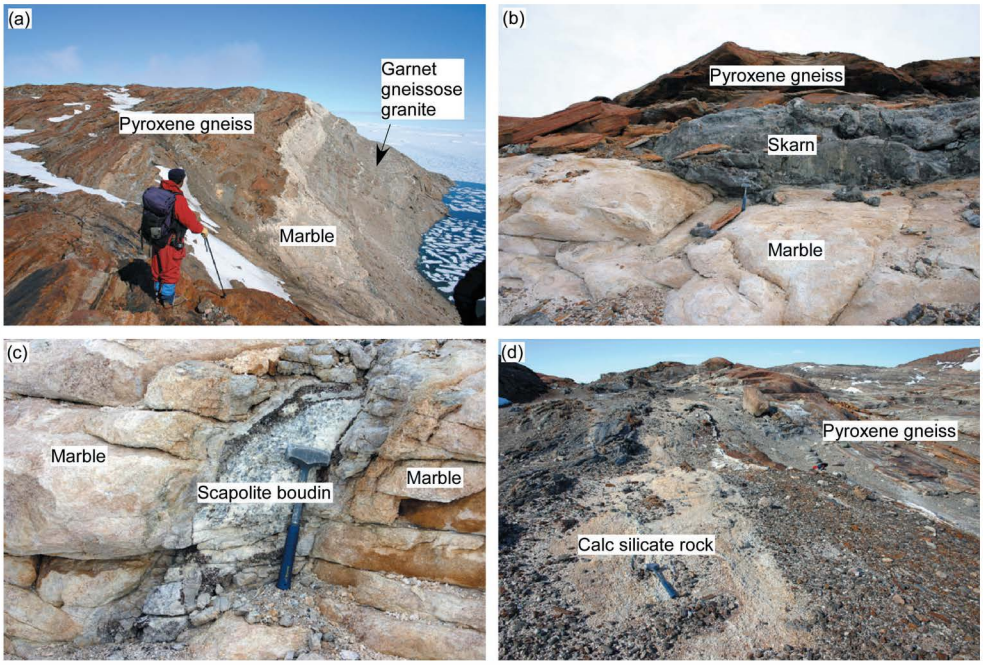

Fig. 5. (a) A general view of the extensive marble layer in Skallevikshalsen. (b) Skarn layers that separate marble and granitic gneiss in the lower contact of the marble layer at Skallevikshalsen. (c) Scapolite boudins in the upper contact zone between marble layer and overlying pelitic gneiss. (d) Calc-silicate layer within the pyroxene gneiss showing garnet+wollastonite+scapolite assemblage.

currences are also observed here. They occur either as meter-scale massive skarn zones between marble (Fig. 5b) and gneiss or as nodules (boudins) up to several meters in diameter or as veins and veinlets completely enclosed within the host marbles (Matsueda *et al.,* 1983). Several decimeter to meter sized scapolite-rich boudins surrounded by phlogopite/amphibole-rich reaction rim were observed within the marble in the upper contact zone of the marble with the gneiss (Fig. 5c).

Apart from marble layers and skarn, a calc-silicate lens of about 5 m long and 2 m thick was observed within the pyroxene gneiss, about 500 m NW of Lake Dairi. This calc-silicate layer comprises of a mineral assemblage of wollastonite＋scapolite＋garnet ＋clinopyroxene in varying proportions near the contact between the lens and the pyroxene-gneiss, whereas the core portions of the lens preserve calcite-rich marble (Fig. 5d). In particular this occurrence is important because of the high concentration of graphite along the contact of calc-silicate rocks and pyroxene gneiss.

4.6. Rundvågshetta

The exposure at Rundvågshetta comprises of compositionally diverse high-temperature granulites including the metapelitic rocks with orthopyroxene-sillimanite-bearing and sapphirine-bearing assemblages (Ishikawa, M. *et al.,* 1994; Motoyoshi and Ishikawa, 1997). Earlier studies have revealed peak metamorphic condition of around 1000°C at *ca.* 11 kbar (Motoyoshi and Ishikawa, 1997). Further evidence for UHT conditions were reported by Yoshimura *et al.* (2003) based on the finding of co-existing sapphirine＋quartz assemblage. The peak metamorphism occurred during the Pan-African Orogeny (517±9 Ma; Fraser *et al*., 2000). Further, Fraser *et al.* (2000), based on a detailed K-Ar and Ar-Ar dating, suggested that the isothermal decompression in the Rundvågshetta region spanned for ~20±10 My, starting at about 520 Ma.

Ishikawa, M. *et al.* (1994) identified early intense deformation in the metamorphic rocks of Rundvågshetta. Based on detailed structural analyses of the region, they suggested that the dominant isoclinal folds and ductile boudinage structures are coeval and represent the regional ductile deformation during the peak metamorphism. In the central region of Rundvågshetta, a 2 m thick boudinaged calc-silicate layer is enclosed in pyroxene gneiss (Fig. 6). The elongate-axes of boudinage are parallel to the general WNW-ESE mineral lineation observed in the host gneisses. A granitic vein intrudes along the lower contact of the boudin and the pyroxene gneiss (Fig. 6).

In general, the calc-silicate assemblage comprises of garnet＋scapolite＋clinopyroxene＋plagioclase＋titanite±calcite±quartz. Although, several mineralogical zones were identified within the boudins, the most distinguishable feature is the presence of zones with garnet porphyroblasts (up to 5 cm) in the core (Fig. 7) and zones where garnet occur as fine intergrowths with scapolite or plagioclase (intermediate zone in Fig. 7). The rim zones are characterized by plagioclase＋clinopyroxene-rich assemblage. The peculiarity of the Rundvågshetta calc-silicate is the absence of granular wollastonite, despite the region being affected by ultrahigh-temperature metamorphic conditions. Instead, wollastonite is present as rare relicts or retrograde intergrowths with plagioclase.

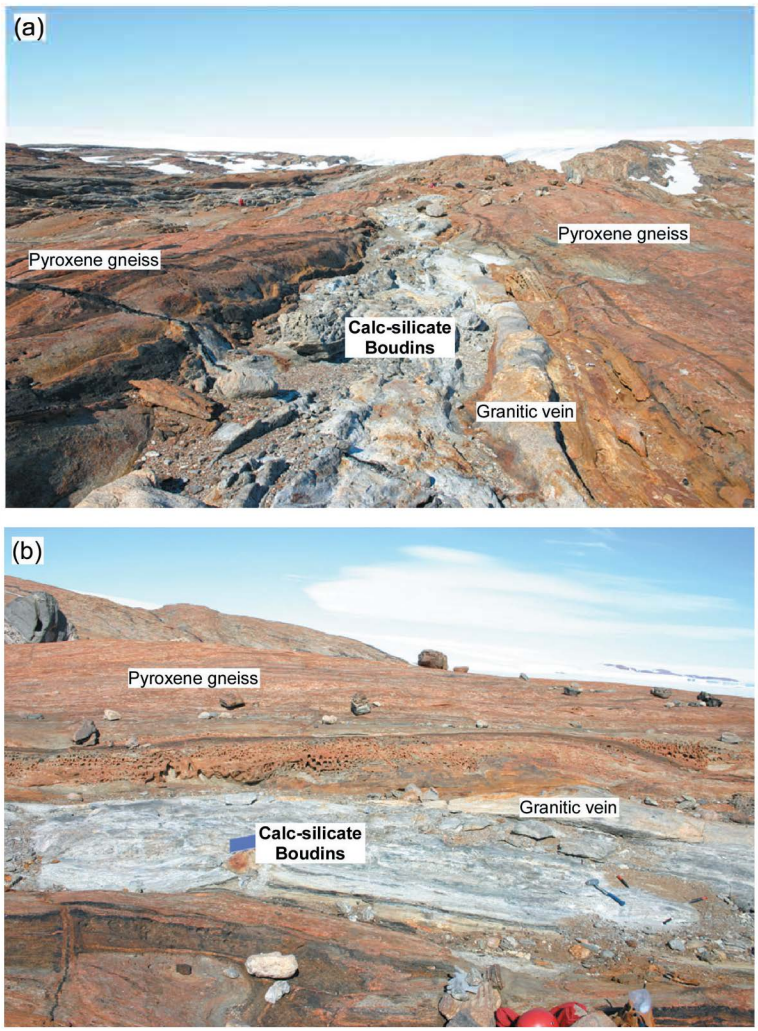

Fig. 6. (a) Field photograph showing the general occurrence of calc-silicate mega-boudins within the pyroxene gneiss at Rundvågshetta. (b) A close-up view of the contact between the calc-silicate boudin and the adjoining gneiss. Note the occurrence of a granitic vein along the contact zone of the calc-silicate boudin.

5. Calc-silicate mega-boudins in Rundvågshetta

We describe here the general mineralogical characteristics and mineral reaction textures observed in the calc-silicate mega-boudins. Based on the mineral chemistry, activity corrected T-X_{CO2} petrogenetic grid was constructed. Preliminary geochemistry of different mineralogical zones is also presented.

5.1. Mineralogy

The mineralogical variation observed within the calc-silicate mega-boudin is clearly

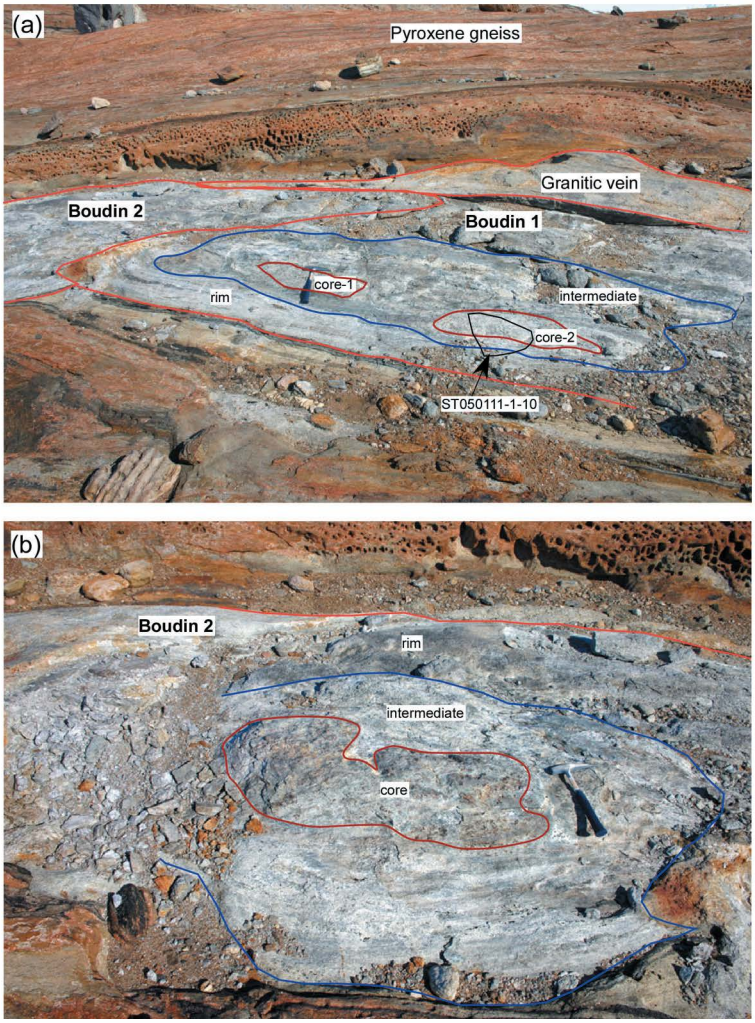

Fig. 7. (a) Field photograph showing different mineralogical zones within the calc-silicate mega-boudin. (b) Sketch of the calc-silicate mega-boudins showing the mineralogical zones and sampling points.

visible in a 50 cm size single hand specimen collected from the boudin (Fig. 8a). Petrography of this sample suggests the presence of distinct mineral zones and domains with corona textures (Fig. 8b), salient features of which are described below. Representative photomicrographs of mineral assemblages and back scatter electron images of reaction textures are shown in Figs. 9 and 10, respectively.

The rim zone of the calc-silicate mega-boudin is characterized by a mineral assemblage of plagioclase + quartz + clinopyroxene. This assemblage commonly shows granular texture. However, occasionally thin aggregates of coarse clinopyroxene are observed. Plagioclase shows concentric zoning with lower anorthite content (An_{60}) in the core (Fig. 9a).

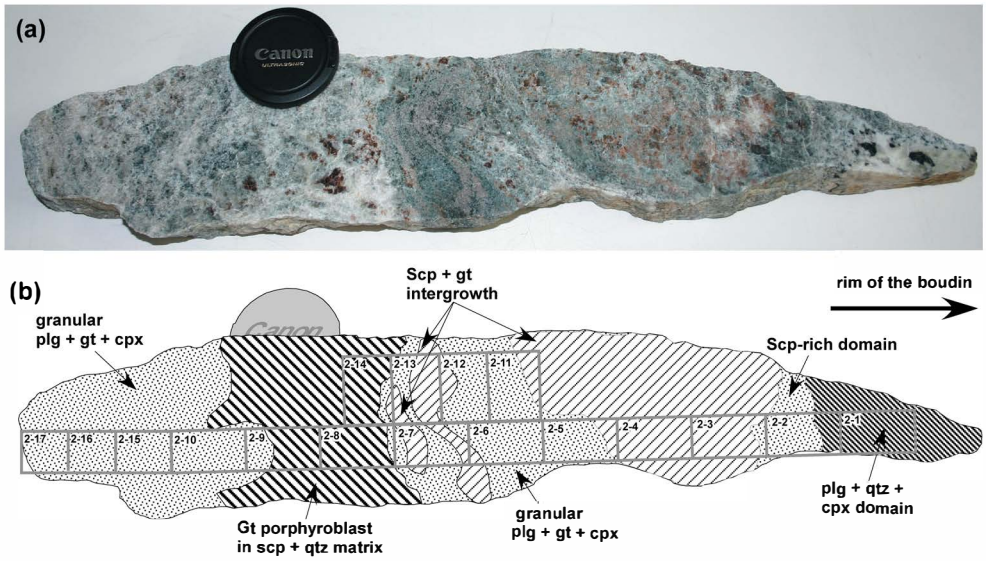

Fig. 8. (a) Cut and polished surface of calc-silicate sample perpendicular to the length of the boudin showing different mineralogical zones. Note the position of thin section for petrologic observations. (b) Sketch of the slab showing the variation in mineral assemblages.

A thin layer of coarse-grained scapolite-rich domain occurs between the rim zone and the intermediate zone. The scapolite-rich domain contains subordinate amounts of quartz and clinopyroxene (Fig. 9b). Intermediate zone comprises of alternating domains of equigranular plagioclase + garnet + clinopyroxene (Fig. 9c, d) and scapolite + garnet intergrowth domain (Fig. 9e, f). Minor amounts of clinopyroxene and titanite occur within these intergrowths.

The core portions of the calc-silicate mega-boudins comprises of garnet porphyroblasts, up to 5 cm in diameter. The matrix comprises of medium grained (up to few millimeters) scapolite + quartz (Fig. 9g), with subordinate amounts of clinopyroxene.

Wollastonite was observed as a relict surrounded by granular calcite and quartz. Titanite is the most common accessory phase found, which shows zoning and overgrowth features(Fig. 9h).

5.2. Reaction textures

Several high temperature metamorphic intergrowths and retrograde reaction textures are observed in the Rundvågshetta calc-silicate rocks. High temperature intergrowth textures of scapolite + grandite garnet ± clinopyroxene and plagioclase + grandite garnet ± clinopyroxene are observed in the intermediate zone. Garnet often shows resorbed grain boundaries and enclosed in larger scapolite grains (Fig. 9e). These intergrowth textures can be considered as symplectites, where mineral reactions have progressed considerably.

Several stages of retrograde reaction textures are identified (Fig. 10). Garnet corona surrounding clinopyroxene (Fig. 10a) or calcite (Fig. 10d) is the prominent one

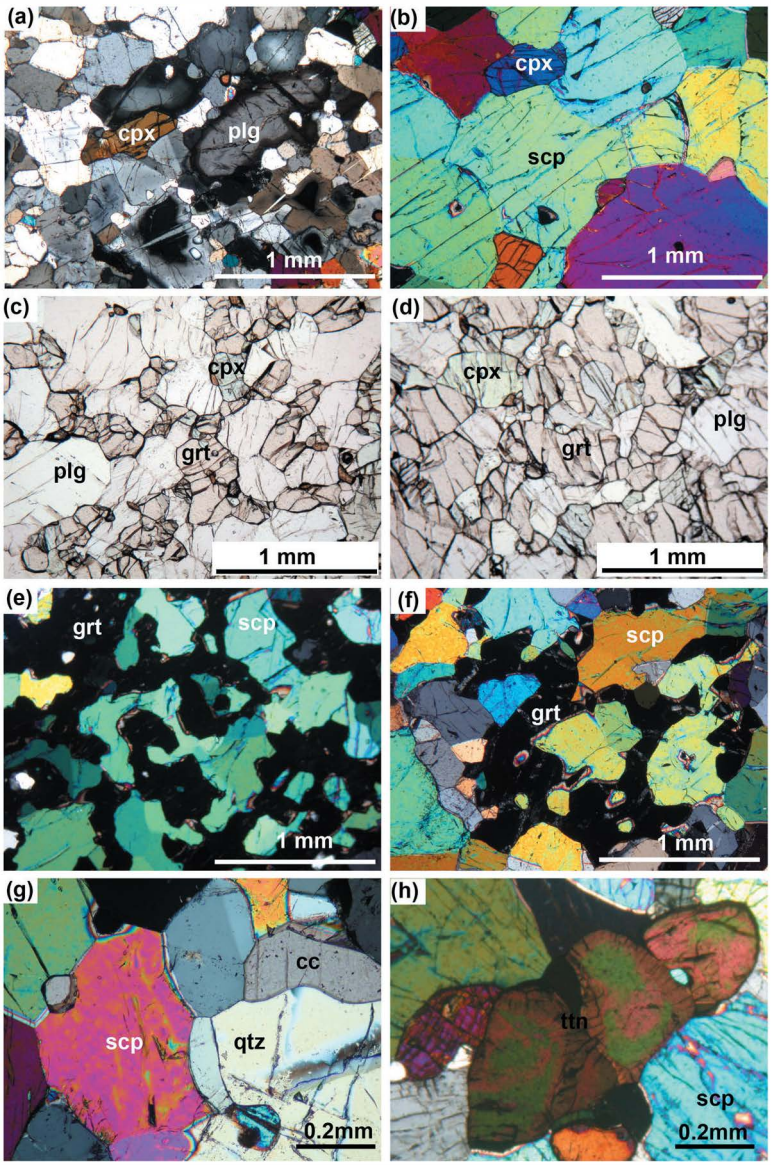

Fig. 9. Thin section photomicrographs depicting representative mineral assemblages observed in different zones in the slab shown in Fig. 8. Photomicrographs are in crossed polars, unless otherwise stated. (a) Zoned plagioclase+clinopyroxene+quartz assemblage observed in the rim of the boudin. (b) Coarse-grained equigranular scapolite-rich assemblage. (c) Granular plagioclase+grandite garnet+clinopyroxene assemblage. (d) Clinopyroxene+grandite garnet dominant zone in the core portion of the boudin. (e) Scapolite+grandite garnet intergrowth commonly observed in the core portions of the boudin. (f) Thick garnet corona texture surrounding scapolite in the core portions of the boudin. (g) Co-existing granular scapolite+quartz+calcite assemblage in the core portions of calc-silicate boudins, where centimeter scale garnet porphyroblast is observed. (h) Zoned titanite associated with scapolite in calc-silicate rocks.

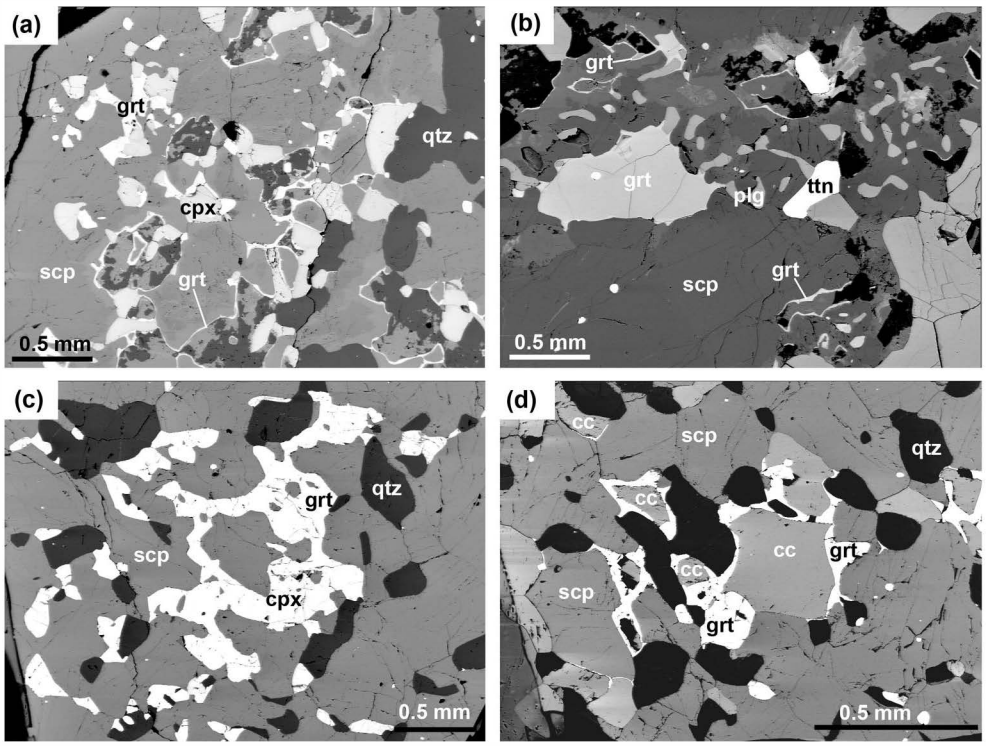

Fig. 10. Backscattered Electron images of some important reaction textures observed in the calc-silicate maga-boudins from Rundvågshetta. (a) (b) (c) Back scattered electron image of scapolite (light gray)+grandite garnet (white) intergrowth. Note the occurrence of quartz (dark gray) as inclusions in scapolite (width of the photograph ~1.5 mm). (d) Back scattered electron image of garnet corona texture observed in calc-silicate rocks of the present study. Scapolite forms the matrix here. The other major phases are clinopyroxene (gray) and quartz (dark gray).

observed. Thin rinds and corona of garnet are also observed surrounding scapolite, partially altered to plagioclase (Fig. 10b). Scapolite in some zones is replaced by plagioclase, calcite and minor amounts of quartz. Wollastonite, found as a relict, is surrounded by retrograde calcite and quartz. Thin rinds of garnet were also observed within the anorthite+calcite±quartz intergrowth, suggesting garnet formation after the breakdown of scapolite.

5.3. Mineral chemistry

Eight thin sections representing major mineralogic zones within the sample ST 050111-1-10 were selected for mineral chemical analysis. Electron microprobe analyses of constituent minerals were carried out using a wave-length dispersive instrument (JEOL-JXA733) housed at Shizuoka University. Measurements were carried out at 15 kV accelerating voltage with a probe current of 0.12 nA at a minimum (~1 μm) beam diameter. Natural and synthetic standards were used as reference materials and Bence and Albee (1968) correction was performed using α factors of Nakamura and Kushiro

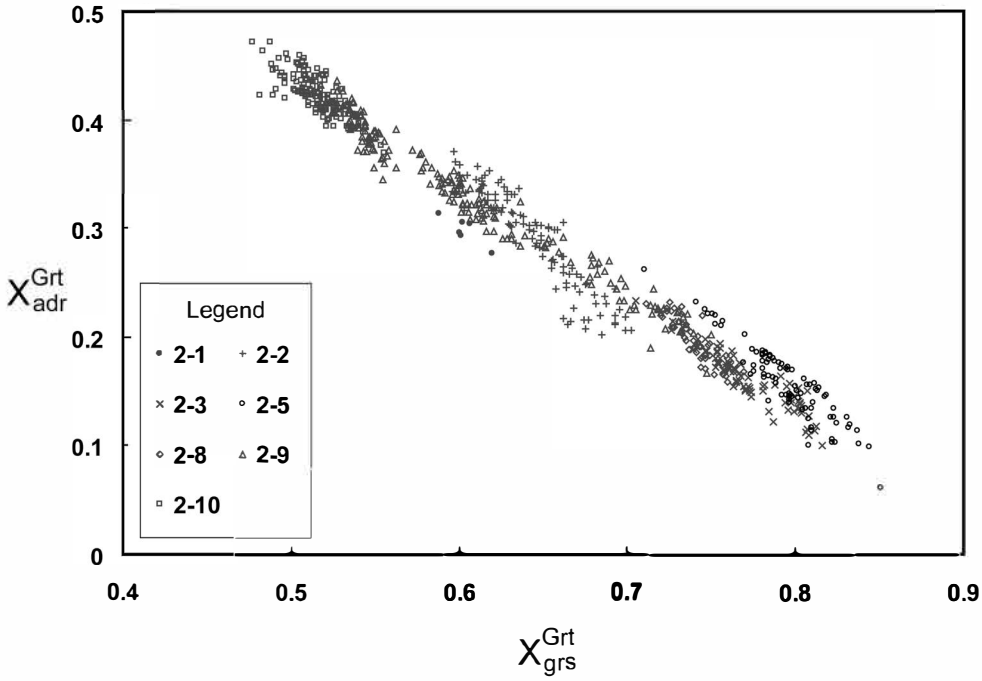

Fig. 11. Compositional variation in garnet observed in a single sample. Sub-sample numbers correspond to those given in Fig. 8b.

(1970). Fe^{3+} in garnet was recalculated by site and charge balance after normalizing the formula to eight cations.

5.3.1 Garnet

Textural features suggest the occurrence of four types of grandite garnet. Garnets are principally grossular-andradite solid solution with minor (< 10 mol%) other components (Fig. 11). Gr_I is porphyroblastic, which is compositionally nearly pure grosssular. Only minor chemical zoning is observed with a decrease in Al content and an increase in Fe^{3+} content toward rim (Table 1). Rims of Gr_I are often replaced by an intergrowth of garnet + plagioclase. Gr_{II} is matrix garnet, coexists with clinopyroxene, anorthite and scapolite, which has andradite component in the range of 5–15%. Gr_{III} forms intergrowth with scapolite and minor clinopyroxene, with andradite component of up to 20%.

Gr_{IV} is garnet formed as corona surrounding other minerals. Texturally there are several types of garnet coronas and in this study we group them together. This type of garnet shows large variation in chemical composition, ranging from almost pure grossular to andradite component up to 50%. Mineral chemical variations within this group are beyond the scope of this paper and will be addressed elsewhere.

5.3.2. Clinopyroxene

Three textural types of clinopyroxene could be identified in Rundvågshetta calc-silicate boudins. Cpx_I is matrix clinopyroxene, which is almost pure diopside (Fig. 12). Cpx_{II} that form thin intergrowth with garnet or scapolite has appreciable CaTs compo-

Table 1. Representative mineral chemistry of garnets in the Rundvågshetta calc-silicate mega-boudin.

Sample	2-2-21	2-2-22	2-2-153	2-2-235	2-5-122	2-5-123	2-5-231	2-5-232	2-6-49	2-6-50	2-8-21	2-9-24	2-9-32	2-10-17	2-10-18
Textural site	Gr_{III}	Gr_{III}	Gr_{IV}	Gr_{IV}	Gr_{II}	Gr_{II}	Gr_{II}	Gr_{II}	Gr_{II}	Gr_{II}	Gr_{I}	Gr_{IV}	Gr_{IV}	Gr_{IV}	Gr_{IV}
SiO_2	38.26	38.41	38.47	37.48	38.69	39.27	38.98	38.90	39.27	39.41	38.70	37.94	37.56	37.24	37.90
TiO_2	0.57	0.58	0.65	0.68	0.67	0.63	0.65	0.65	0.73	0.73	0.65	0.72	0.69	0.70	0.70
Al_2O_3	16.83	16.21	14.10	14.87	18.38	18.72	17.95	19.79	18.88	18.45	18.18	13.16	13.00	12.39	12.33
Cr_2O_3	0.14	0.14	0.14	0.17	0.14	0.16	0.13	0.11	0.16	0.17	0.17	0.12	0.11	0.15	0.15
$Fe_2O_3^{\#}$	9.22	8.65	11.14	11.97	4.89	4.21	4.89	4.15	3.83	4.08	7.84	12.85	13.54	15.61	14.88
FeO	0.92	1.90	1.77	0.32	1.11	1.67	0.83	0.65	1.91	1.79	0.34	1.30	1.17	0.21	0.87
MnO	0.78	0.71	0.71	0.53	0.61	0.65	0.58	0.61	0.72	0.67	0.64	0.79	0.77	0.73	0.75
MgO	0.27	0.26	0.27	0.26	0.42	0.34	0.37	0.45	0.61	0.50	0.52	0.25	0.24	0.23	0.23
CaO	33.88	33.35	33.51	33.92	34.12	34.30	34.70	34.58	33.53	34.17	34.57	33.43	33.11	33.66	33.70
Na_2O	0.08	0.07	0.09	0.07	0.09	0.08	0.08	0.10	0.14	0.08	0.09	0.08	0.09	0.08	0.08
K_2O	0.09	0.10	0.10	0.10	0.09	0.10	0.09	0.09	0.09	0.09	0.08	0.09	0.11	0.10	0.11
Total	101.05	100.38	100.93	100.37	99.20	100.11	99.26	100.07	99.87	100.14	101.80	100.74	100.39	101.12	101.71
Cations on the basis of 12 oxygen															
Si	2.943	2.979	2.995	2.929	2.989	3.004	3.009	2.963	3.006	3.014	2.933	2.976	2.962	2.928	2.960
Ti	0.033	0.034	0.038	0.040	0.039	0.036	0.038	0.037	0.042	0.042	0.037	0.042	0.041	0.042	0.041
Al	1.526	1.482	1.295	1.370	1.674	1.688	1.634	1.778	1.704	1.663	1.624	1.217	1.208	1.149	1.136
Cr	0.009	0.009	0.009	0.011	0.009	0.009	0.008	0.007	0.010	0.010	0.010	0.008	0.007	0.009	0.009
$Fe^{3+\#}$	0.534	0.505	0.653	0.704	0.284	0.242	0.284	0.238	0.221	0.235	0.447	0.759	0.803	0.924	0.875
Fe^{2+}	0.059	0.124	0.115	0.021	0.072	0.107	0.054	0.041	0.122	0.114	0.022	0.085	0.077	0.014	0.057
Mn	0.051	0.047	0.047	0.035	0.040	0.042	0.038	0.039	0.047	0.043	0.041	0.053	0.051	0.049	0.050
Mg	0.031	0.030	0.031	0.030	0.048	0.039	0.043	0.051	0.070	0.057	0.058	0.029	0.029	0.027	0.027
Ca	2.793	2.771	2.796	2.840	2.824	2.811	2.871	2.823	2.750	2.800	2.807	2.810	2.797	2.836	2.821
Na	0.012	0.011	0.013	0.011	0.013	0.011	0.012	0.014	0.021	0.012	0.013	0.012	0.013	0.012	0.013
K	0.009	0.010	0.009	0.010	0.008	0.010	0.008	0.009	0.009	0.009	0.008	0.009	0.011	0.010	0.011
Total	8.000	8.000	8.000	8.000	8.000	8.000	8.000	8.000	8.000	8.000	8.000	8.000	8.000	8.000	8.000
Mg#	0.34	0.19	0.21	0.59	0.40	0.27	0.44	0.55	0.36	0.33	0.73	0.25	0.27	0.66	0.32
Pyrope	0.01	0.01	0.01	0.01	0.02	0.01	0.01	0.02	0.02	0.02	0.02	0.01	0.01	0.01	0.01
Almandine	0.02	0.04	0.04	0.01	0.02	0.04	0.02	0.01	0.04	0.04	0.01	0.03	0.03	0.00	0.02
Spessartine	0.02	0.02	0.02	0.01	0.01	0.01	0.01	0.01	0.02	0.01	0.01	0.02	0.02	0.02	0.02
Grossular	0.68	0.67	0.60	0.62	0.80	0.81	0.80	0.83	0.80	0.80	0.73	0.55	0.54	0.51	0.51
Andradite	0.27	0.26	0.33	0.35	0.15	0.12	0.15	0.12	0.11	0.12	0.22	0.39	0.41	0.46	0.44

calculated

nent (Al$<$0.5 afpu). Cpx_{III} are inter-grown with garnet and has slightly higher hedenbergite content (Table 2).

5.3.3. Scapolite

Compositional variation in scapolite is usually expressed in EqAn content (EqAn$=$1–Al/(Al–3); Al calculated from analyses normalized to Si$+$Al$=$12 cations; Evans *et al*., 1969). In this study, we found the scapolite compositions are meionite-rich, with EqAn values in the range between 75 and 90. Scapolite co-existing with anorthite has higher EqAn values between 80 and 90 (Fig. 13), whereas scapolite without co-existing plagioclase has lower EqAn values between 75 and 85 (Table 3).

5.3.4. Plagioclase

There are two generations of plagioclase observed in the calc-silicate boudins. First type is the granular type which co-exists with all other major minerals. The second type is texturally late plagioclase type could be identified as products of retrogression of scapolite. However, both textural types of plagioclase are anorthite-rich in chemical composition ($>An_{90}$; Fig. 13). Plagioclase in the contact zone between boudin and the

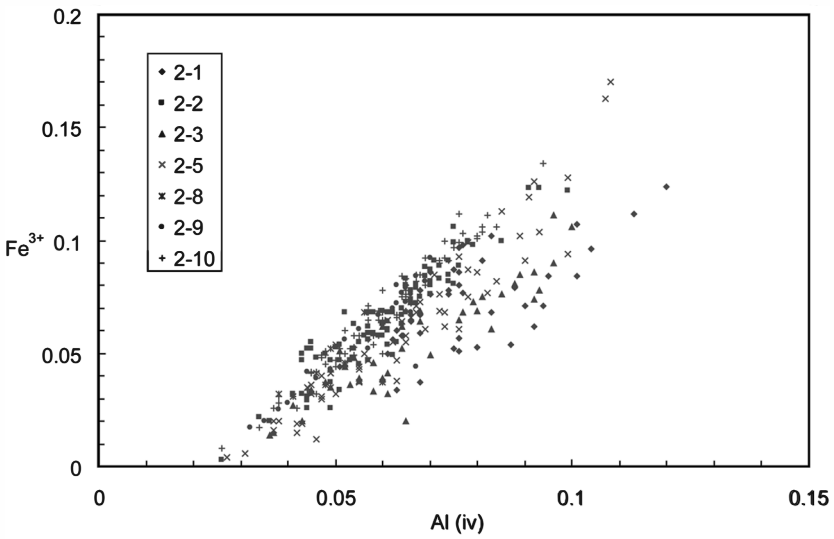

Fig. 12. A plot of octahedral Fe^{3+} versus tetrahedral Al for clinopyroxene.

Table 2. Mineral chemistry of clinopyroxene in the Rundvågshetta calc-silicate mega-boudin.

Sample	2-1-78	2-1-80	2-2-207	2-2-208	2-5-163	2-9-212	2-10-228
SiO_2	54.56	52.90	50.47	50.82	52.12	50.29	49.67
TiO_2	0.46	0.44	0.33	0.32	0.32	0.37	0.34
Al_2O_3	2.59	3.69	1.44	1.42	2.04	1.29	1.20
Cr_2O_3	0.15	0.09	0.14	0.16	0.14	0.12	0.14
$Fe_2O_3^{\#}$	0.00	0.00	3.11	3.45	0.00	2.51	3.55
FeO	12.10	13.19	11.43	11.29	7.11	14.13	14.38
MnO	0.49	0.48	0.61	0.61	0.47	0.94	1.04
MgO	16.86	15.34	9.18	9.19	12.46	7.10	6.56
CaO	12.76	12.73	23.97	24.34	24.61	24.25	24.07
Na_2O	0.29	0.32	0.27	0.28	0.22	0.29	0.31
K_2O	0.20	0.32	0.09	0.09	0.09	0.09	0.09
Total	100.46	99.50	101.03	101.96	99.58	101.37	101.35
Cations on the basis of 6 oxygens							
Si	1.992	1.965	1.924	1.921	1.954	1.935	1.923
Ti	0.013	0.012	0.009	0.009	0.009	0.011	0.010
Al	0.111	0.162	0.065	0.063	0.090	0.058	0.055
Cr	0.004	0.003	0.004	0.005	0.004	0.003	0.004
Fe^{3+}	0.000	0.000	0.089	0.098	0.000	0.073	0.103
Fe^{2+}	0.369	0.410	0.364	0.357	0.223	0.455	0.466
Mn	0.015	0.015	0.020	0.020	0.015	0.031	0.034
Mg	0.918	0.849	0.522	0.518	0.696	0.407	0.378
Ca	0.499	0.507	0.979	0.986	0.989	1.000	0.999
Na	0.020	0.023	0.020	0.021	0.016	0.022	0.023
K	0.009	0.015	0.004	0.004	0.004	0.005	0.004
Sum	3.952	3.960	4.000	4.000	4.000	4.000	4.000
Mg#	0.71	0.67	0.59	0.59	0.76	0.47	0.45
Di	0.94	0.91	0.87	0.87	0.94	0.86	0.83
CaTs	0.06	0.09	0.05	0.05	0.06	0.06	0.06
FeTs	0.00	0.00	0.07	0.08	0.00	0.08	0.11

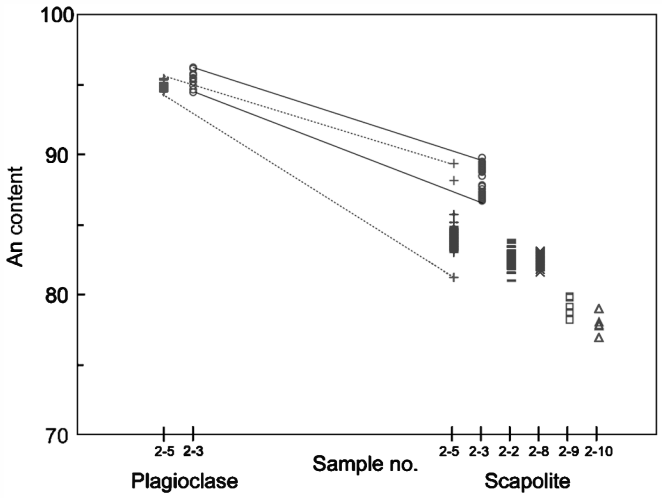

Fig. 13. Compositional variations in co-existing scapolite and plagioclase.

Table 3. Scapolite and plagioclase mineral chemistry in the calc-silicate mega-boudin in Rundvågshetta.

Sample	2-1-14	2-1-18	2-1-28	2-1-97	2-3-141	2-3-142	2-3-104	2-5-36	2-5-37	2-8-122
Textural site	Plg-rim	Plg-core	Plg-rim	Plg-core	Plg-core	Plg-rim	scap	scap	scap	scap
SiO_2	46.85	53.48	46.8	52.79	44.14	44.6	42.43	43.67	44.27	44.5
TiO_2	0.24	0.25	0.26	0.23	0.24	0.26	0.23	0.25	0.25	0.24
Al_2O_3	34.62	30	33.8	31.34	35.27	36.08	29.91	27.3	28.04	27.61
Cr_2O_3	0.17	0.13	0.11	0.13	0.17	0.08	0.12	0.09	0.11	0.17
FeO	0.39	0.35	0.4	0.33	0.32	0.26	0.35	0.32	0.35	0.41
MnO	0.14	0.13	0.11	0.13	0.14	0.14	0.14	0.13	0.17	0.17
MgO	0.08	0.08	0.08	0.07	0.07	0.07	0.14	0.13	0.13	0.15
CaO	17.4	12.54	16.99	13.86	20.03	19.8	21.71	19.98	20.04	19.93
Na_2O	1.62	4.28	1.97	3.77	0.36	0.49	1.28	1.75	1.84	1.99
K_2O	0.16	0.44	0.18	0.22	0.1	0.1	0.29	0.41	0.4	0.48
Total	101.67	101.68	100.7	102.87	100.85	101.89	96.6	94.05	95.58	95.64
Cations on the basis of 8 oxygen							Calculated on the basis of total 16 cations			
Si	2.124	2.39	2.142	2.337	2.033	2.03	6.485	6.848	6.826	6.854
Ti	0.008	0.008	0.009	0.008	0.008	0.009	0.027	0.029	0.029	0.027
Al	1.85	1.581	1.824	1.635	1.915	1.936	5.389	5.047	5.098	5.014
Cr	0.006	0.005	0.004	0.005	0.006	0.003	0.014	0.012	0.013	0.02
Fe	0.013	0.012	0.014	0.011	0.011	0.009	0.045	0.042	0.045	0.053
Mn	0.005	0.005	0.004	0.005	0.006	0.006	0.017	0.017	0.022	0.022
Mg	0.005	0.005	0.006	0.005	0.005	0.005	0.032	0.031	0.029	0.034
Ca	0.845	0.6	0.833	0.657	0.988	0.966	3.555	3.357	3.311	3.288
Na	0.142	0.371	0.175	0.324	0.033	0.043	0.379	0.533	0.549	0.594
K	0.009	0.025	0.011	0.012	0.006	0.006	0.057	0.083	0.079	0.094
Total	5.008	5.001	5.021	4.998	5.011	5.012	16	16	16	16
An	0.85	0.60	0.82	0.66	0.96	0.95				
Ab	0.14	0.37	0.17	0.33	0.03	0.04				
EqAn							89.1	84.5	84.0	82.7

country gneiss shows chemical zoning, with anorthite-rich rim (An_{87}) and less anorthitic cores (An_{72}) (Table 3).

5.4. Geochemistry

Whole rock chemical composition from the contact toward the core for distance of about 50 cm. Whole-rock compositions of major elements were determined using a

Table 4. Results of bulk rock chemistry of various zones of calc-silicate mega-boudin.

Sample	10-2-1	10-2-2	10-2-3	10-2-4	10-2-5	10-2-6	10-2-7	10-2-8	10-2-9	10-2-10	10-2-11	10-2-12
SiO_2	64.00	62.62	47.61	46.21	48.58	44.72	45.65	64.54	64.96	53.89	57.56	50.52
TiO_2	0.10	0.17	0.20	0.23	0.16	0.28	0.33	0.17	0.03	0.03	0.13	0.11
Al_2O_3	18.39	18.48	24.95	25.16	24.00	25.88	23.20	19.16	19.69	20.86	19.31	22.22
Fe_2O_3 (total)	1.66	1.68	2.18	2.49	2.76	3.21	3.60	1.13	0.59	0.88	2.39	1.19
MnO	0.06	0.07	0.09	0.12	0.15	0.15	0.19	0.06	0.03	0.04	0.12	0.07
MgO	1.07	0.78	1.26	1.37	1.55	3.19	4.66	0.57	0.47	0.29	0.57	0.44
CaO	12.07	14.68	22.17	23.01	21.40	23.31	23.86	14.33	12.62	17.94	17.81	19.74
Na_2O	2.10	1.41	1.33	1.30	1.36	0.15	0.12	1.23	0.97	1.85	1.24	1.73
K_2O	0.56	0.13	0.22	0.21	0.23	0.20	0.12	0.29	0.19	0.48	0.29	0.34
P_2O_5	0.13	0.05	0.07	0.08	0.07	0.11	0.11	0.05	0.03	0.04	0.04	0.03
LOI	0.71	0.39	0.40	0.33	0.25	0.44	0.27	0.69	0.33	3.25	0.37	3.02
Total	100.85	100.46	100.48	100.52	100.49	101.64	102.11	102.21	99.90	99.55	99.84	99.40

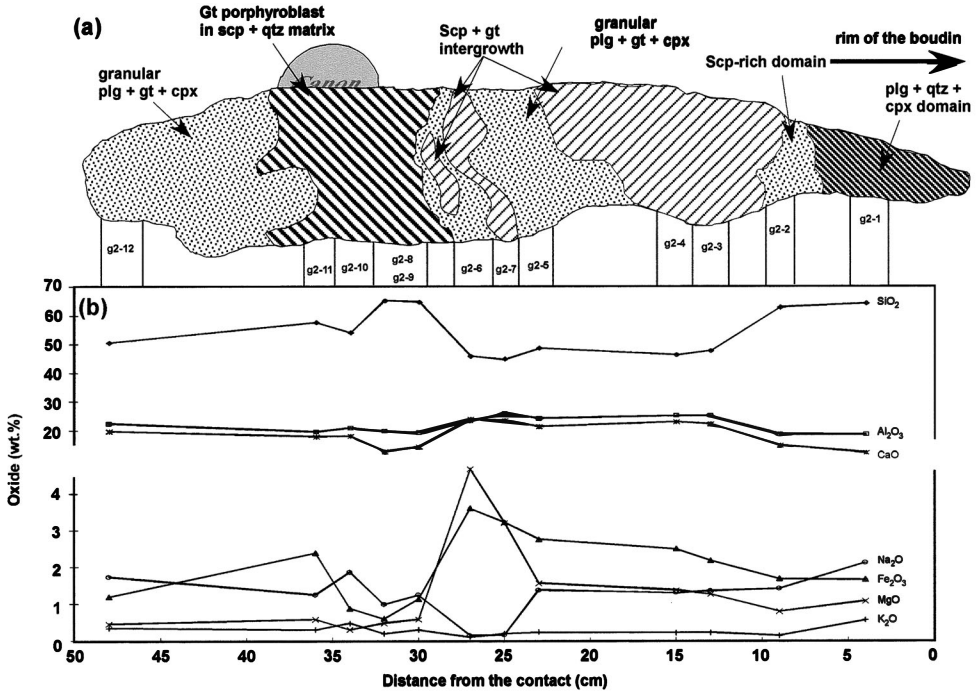

Fig. 14. Major element distribution diagram showing the trend of some major elements from the rim of the calc-silicate mega-boudin toward core.

Rigaku X-ray fluorescence spectrometer (XRF) at the National Institute of Polar Research (NIPR) following the analytical procedures described in Motoyoshi and Shiraishi (1994). Representative whole-rock compositions are listed in Table 4, where LOI contents are included into the total weight percent of the major oxides.

Major element variation from the boudin rim toward core, shown in Fig. 14, is characterized by chemical gradient corresponding to the mineral assemblage zones. It is evident that the zones where quartz is observed in excess, have silica content of about 60 wt%, except samples g2-10 and g2-11 that contain garnet porphyroblasts. These zones are also characterized by low CaO and Al_2O_3 contents, whereas no significant variation is observed in other elements. Appreciable increase in MgO and Fe_2O_3 is observed in the zone having higher modal clinopyroxene and garnet (samples g2-6 and g2-7). Samples having higher calcite content consistently gave higher LOI contents. The possibility of H_2O^+ contributing to the LOI content can be ignored since hydrous minerals are absent in the calc-silicate rocks.

6. Discussion

6.1. Deducing peak metamorphic P-T-fluid conditions of the Rundvågshetta region

Coexisting scapolite and plagioclase is sensitive to temperature and therefore scapolite phase equilibria provides a mean to estimate the minimum metamorphic temperature condition (Ellis, 1978; Moecher and Essene, 1990). The vapor absent equilibria Scp = 3An + Cc, between coexisting plagioclase and scapolite (Fig. 13), suggests minimum temperature of formation of scapolite around ~830°C. This minimum estimate is supportive of the ultrahigh-temperature peak metamorphic conditions recorded in the metapelitic rocks (~1000°C; Motoyoshi and Ishikawa, 1997).

Grandite garnet + scapolite and grandite garnet + plagioclase intergrowth with subordinate amounts of clinopyroxene is commonly found in the intermediate portions of the boudins. In addition, co-existing scapolite + quartz and calcite + quartz assemblages are also observed. These assemblages suggest that a high-pressure and/or high-X_{CO2} conditions prevailed during peak metamorphism (Harley and Buick, 1992). Computation of T-X_{CO2} partial petrogenetic grid for the peak metamorphic assemblage was carried out using an internally consistent thermodynamic data set of Holland and Powell (1998) employing the computer software THERMOCALC v.3.1 (Powell and Holland, 2001). Measured mineral compositions of garnet and scapolite were used for activity computations following the procedure described in Harley and Buick (1992). The grid was constructed at a pressure condition of 11 kbar, considered as optimum for Rundvågshetta region (Motoyoshi and Ishikawa, 1997). In the simplified CASV system (Mg and Fe-free), the scapolite-dominant wollastonite-free assemblage should have equilibrated at moderate to high X_{CO2} conditions (0.3–0.7) and temperatures between 850 and 1000°C (Fig. 15). Relict wollastonite is indicative of either high temperature conditions or low X_{CO2} fluid composition. The plagioclase-dominant (wollastonite-, calcite-absent) assemblages indicate the X_{CO2} conditions at peak P-T might have been low to moderate (< 0.45).

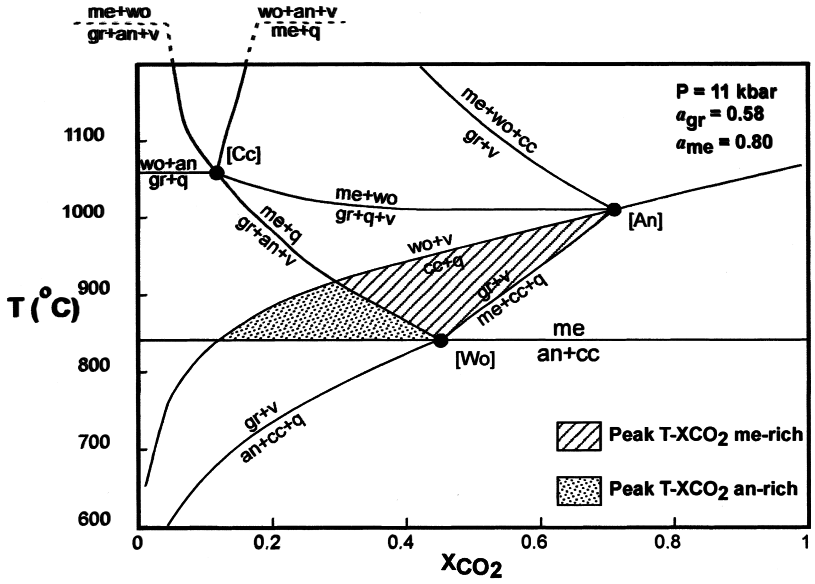

Fig. 15. T-X_{CO2} diagram showing the possible temperature condition and the range of fluid composition during the peak metamorphism of the Rundvågshetta calc-silicate mega-boudins. Note that temperature range observed is minimum temperature for equilibration of the observed calc-silicate assemblage.

6.2. Retrograde P-T-fluid evolution

Although a rigorous petrogentic analysis based on the chemical composition of garnet with respect to various textures is necessary to evaluate the retrograde *P-T-X* conditions of Rundvågshetta calc-silicate mega-boudins, preliminary results indicate that the garnet corona formation resulted due to an increment in the hydrous component in the fluid during retrogression. Further, scapolite breakdown occurred during cooling (*e.g.* Harley and Buick, 1992), whereas subsequent garnet corona formation resulted from an increase in hydrous component in the fluid. It remains a topic for future studies to determine the temporal and spatial relation of this retrograde fluid compositional fluctuation observed in the calc-silicate rocks with the intrusion of granitic vein along the contact of the calc-silicate boudin and the country rocks.

6.3. Diffusive transfer of elements during UHT metamorphism

Mineralogic zones which are largely concentric to the shape of the boudin suggest diffusive movement of major elements between the boudin and the country rocks. Chemical compositional variations are consistent with the high-variance mineral assemblage of clinopyroxene + plagioclase in the rim portions of boudins and gradnite garnet + scapolite in the core portions of the boudins. Such zoned calc-silicate assemblages are common in high-grade terranes, such as those reported in Rauer Group, East Antarctica (Buick *et al.*, 1993) and contact zones between marbles and pelites (*e.g.* Glassley, 1983). Mass transfer between the calcareous and siliceous protoliths by diffusional exchange is a commonly recommended mechanism during high-grade meta-

morphism. The key physical factors that play a role in such a diffusional process are temperature condition and the presence of fluids that help in the movement of elements across the contact between lithological units. With the present scale of investigation it is possible to conclude that the rim portions of the calc-silicate boudins were affected by diffusional exchange of elements, though the length-scale and patterns remain unclear.

Within the intermediate and core zone of the Rundvågshetta calc-silicate mega-boudins, the chemical potential gradients of major elements are nominal. In other words, it can be stated that the internal diffusional exchange of elements were less pronounced within the boudin. Therefore, the chemical variations perhaps indicate the preservation of original protolith geochemical signatures. The variations in the mineral assemblages suggest that calc-silicate rocks were able to preserve the layer controlled chemical potentials even at UHT metamorphic conditions.

6.4. Regional significance of calc-silicate rocks and marbles

In addition to the sporadic occurrences of calc-silicate rocks and marbles reported in Hiroi *et al.* (1987), the present study identified several new occurrences in the LHC. Based on the paragenetic variations and reaction relations, Hiroi *et al.* (1987) identified a regional southwestward increase in metamorphic conditions in the LHC. The mode of occurrence and mineralogical features observed in the calc-silicate rocks and marbles in the present study are in agreement with the existing regional pressure-temperature gradient. In addition, the new occurrences are considered to contribute in refining the regional metamorphic fluid composition and its evolution. Especially, the present study focused on the occurrence and mineralogical features of calc-silicate rock in the ultrahigh temperature metamorphosed Rundvågshetta region. Moderate to high X_{CO2} conditions (up to 0.7) observed during peak metamorphism at Rundvågshetta is in concurrence with the general trend of increasing X_{CO2} conditions with an increase in metamorphic temperature reported in Hiroi *et al.* (1987). However, the mineralogical and geochemical features warrant the need for a detailed petrologic evaluation of the UHT metamorphosed calc-silicate rocks. Furthermore, the recent finding of carbonation of Cl-rich scapolite boudins from Skallen (Satish-Kumar *et al*., 2006a) and identical occurrences reported in this study from Skallevikshalsen suggest an important role of volatile phases during the metamorphic evolution of the terrain. Thus, the occurrence of calc-silicate rocks and marbles throughout the eastern Dronning Maud Land can enlighten our understanding on the regional *P-T*-fluid regime during the Pan-African tectonothermal event.

Acknowledgments

Dr. Naoto Ishikawa is thanked for his advices, support and kind helps (and patience) offered during the JARE-46 field expedition. Drs. T. Kawakami and T. Tsunogae are thanked for giving some good suggestions to improve the manuscript. We thank Mr. T. Ogino and Mr. M. Takai "*Little Blue*" (helicopter) logistics. The logistics provided by the ice-breaker "*Shirase*" crew and the support from JARE-46 members helped in successfully completing the geological field expedition. We also would like to express our sincere gratitude to JARE-46 leader Mr. Kouji Matsubara and

sub-leader Mr. Hideaki Otsuka for support. Mr. Hideki Mori is thanked for preparing thin sections in a short notice. MS-K acknowledges grants from the Ministry of Education, Culture, Sports, Science and Technology, Japan (Nos. 15740302 & 18740319).

References

Bence, A.E. and Albee, A.L. (1968): Empirical correction factors for the electron microanalysis of silicates and oxides. J. Geol., **76**, 382–403.

Buick, I.S., Harley, S.L. and Cartwright, I.C. (1993): Granulite facies metasomatism: zoned calc-silicate boudins from the Rauer Group, East Antarctica. Contrib. Mineral. Petrol., **113**, 557–571.

Buick, I.S., Cartwright, I.C., Hand, M. and Powell, R. (1994): Evidence for pre-regional metamorphic fluid infiltration of the Lower Calcsilicate Unit, Reynolds Range Group (central Australia). J. Metamorph. Geol., **12**, 789–810.

Buick, I.S., Cartwright, I. and Williams, I.S. (1997): High-temperature retrogression of granulite-facies marbles from Reynolds Range Group, central Australia: Phase equilibria, isotopic resetting and fluid fluxes. J. Petrol., **38**, 877–910.

Cartwright, I. and Valley, J.W. (1991): Steep oxygen-isotope gradients at marble-metagranite contacts in the northwest Adirondack Mountains, New York, USA: product of fluid-hosted diffusion. Earth Planet. Sci. Lett., **107**, 148–163.

Dasgupta, S. and Pal, S. (2005): Origin of grandite garnet in calc-silicate granulites: mineral-fluid equilibria and petrogenetic grids. J. Petol., **46**, 1045–1076.

Ellis, D.E. (1978): Stability and phase equilibria of the chloride and carbonate bearing scapolites at 750℃ and 4000 bars. Geochim. Cosmochim. Acta, **42**, 1271–1281.

Evans, B.W., Shaw, D.M. and Houghton, D.R. (1969): Scapolite stoichiometry. Contrib. Mineral. Petrol., **24**, 293–305.

Ferry, J.M. (1992): Regional metamorphism of the Waits River Formation, eastern Vermount: delineation of a new type of giant metamorphic hydrothermal system. J. Petrol., **33**, 45–94.

Ferry, J.M., Sorensen, S.S. and Rumble, D., III (1998): Structurally controlled fluid flow during contact metamorphism in the Ritter Range pendant, California, USA. Contrib. Mineral. Petrol., **130**, 358–378.

Fitzsimons, I.C.W. and Harley, S.L. (1995): Garnet coronas in scapolite-wollastonite calc-silicates from East Antarctica: the application and limitations of activity-corrected grids. J. Metamorph. Geol., **12**, 761–777.

Fraser, G., McDougall, I., Ellis, D.J. and Williams, I.S. (2000): Timing and rate of isothermal decompression in Pan-African granulites from Rundvågshetta, East Antarctica. J. Metamorph. Geol., **18**, 441–454.

Glassley, W.E. (1983): Deep crustal carbonates as CO_2 fluid sources-evidence from metasomatic reaction zones. Contrib. Mineral. Petrol., **84**, 15–24.

Harley, S.L. and Buick, I.S. (1992): Wollastonite-scapolite assemblages as indicators of granulite pressure-temperature-fluid histories: the Rauer Group, East Antarctica. J. Petrol., **33**, 693–728.

Harley, S.L., Fitzsimons, I. and Buick, I.S. (1994): Reactions and textures in wollastonite-scapolite granulites and their significance for pressure temperature fluid histories of high grade terranes. Precambrian Res., **66**, 309–323.

Hiroi, Y. and Kojima, H. (1988): Petrology of dolomitic marbles from Kasumi Rock, Prince Olav Coast, East Antarctica. Proc. NIPR Symp. Antarct. Geosci., **2**, 96–109.

Hiroi, Y., Shiraishi, K., Yanai, K. and Kizaki, K. (1983): Aluminum silicates in the Prince Olav and Sôya Coasts, East Antarctica. Mem. Natl Inst. Polar Res., Spec. Issue, **28**, 115–131.

Hiroi, Y., Shiraishi, K., Motoyoshi, Y., Kanisawa, S., Yanai, K. and Kizaki, K. (1986): Mode of occurrence, bulk chemical compositions, and mineral textures of ultramafic rocks in the Lützow-Holm Complex, East Antarctica. Mem. Natl Inst. Polar Res., Spec. Issue, **43**, 62–84.

Hiroi, Y., Shiraishi, K., Motoyoshi, Y. and Katsushima, T. (1987): Progressive metamorphism of calc-silicate rocks from the Prince Olav and Sôya Coasts, East Antarctica. Proc. NIPR Symp. Antarct. Geosci.,

1, 73–97.

Hiroi, Y., Shiraishi, K. and Motoyoshi, Y. (1991): Late Proterozoic paired metamorphic complexes in East Antarctica, with special reference to the tectonic significance of ultramafic rocks. Geological Evolution of Antarctica, ed. by M.R.A. Thomson *et al*. Cambridge, Cambridge University Press, 83–87.

Hiroi, Y., Motoyoshi, Y., Ishikawa, N., Satish-Kumar, M., Kagashima, S. and Suda, Y. (2005): Granulite-facies metamorphism in the Cape Hinode area, Prince Olav Coast, East Antarctica. The 25th Symposium on Polar Geosciences, Program and Abstarcts, 13–14 October 2005. Tokyo, Natl Inst. Polar Res., 37 (in Japanese).

Holland, T.J.B. and Powell, R. (1998): An internally consistent thermodynamic data set for phases of petrologic interest. J. Metamorph. Geol., **16**, 309–343.

Ikeda, T. and Kawakami, T. (2004): Structural analysis of Lützow-Holm Complex in Akarui Point, East Antarctica, and overview of the complex. Polar Geosci., **17**, 22–34.

Ishikawa, T. (1976): Superimposed folding of the Precambrian metamorphic rocks of the Lützow-Holm Bay region, East Antarctica. Mem. Natl Inst. Polar Res., Ser. C (Earth Sci.), **9**, 41 p.

Ishikawa, T., Yanai, K., Matsumoto, Y., Kizaki, K., Kojima, S., Tatsumi, T., Kikuchi, T. and Yoshida, M. (1977): Geologcial map of Skarvsnes, Antarctia. Antarctic Geological Map Series, Sheet 6 and 7 (with explanatory text 10 p.). Tokyo, Natl Inst. Polar Res.

Ishikawa, M., Motoyoshi, Y., Fraser, G.L., Kawasaki, T. (1994): Structural evolution of Rundvågshetta region, Lützow-Holm Bay region, East Antarctica. Proc. NIPR Symp. Antarct. Geosci., **7**, 69–89.

Kawakami, T. and Motoyoshi, Y. (2004): Timing of attainment of spinel+quartz coexistence in the garnet-sillimanite leucogneiss from Skallevikshalsen, Lützow-Holm Complex, East Antarctica. J. Mineral. Petrol. Sci., **99**, 311–319.

Klemd, R., Matthes, S. and Schussler, U. (1994): Reaction textures and fluid behaviour in the very high pressure calc-silicate rocks of the Munchberg gneiss complex, Bavaria, Germany. J. Metamorph. Geol., **12**, 735–745.

Kusachi, I., Osanai Y., Toyoshima, T., Owada, M., Tsunogae, T., Hokada, T. and Crowe, W.A. (1999): Mineralogy of scapolite from Skallen in the Lützow Holm Bay region, East Antarctica. Polar Geosci., **12**, 143–156.

Matsueda, H., Motoyoshi, Y. and Matsumoto, Y. (1983): Mg-Al skarn of the Skallevikshalsen on the east coast of Lützow-Hom Bay, East Antarctica. Mem. Natl Inst. Polar Res., Spec. Issue, **28**, 166–182

Moecher, D.P. and Essene, E.J. (1990): Phase equilibria for calcic scapolite, and implications of variable Al-Si disorder for *P-T, T-*X_{CO2}, and *a-X* relations. J. Petrol., **31**, 997–1024.

Motoyoshi, Y. and Ishikawa, M. (1997): Metamorphic and structural evolution of granulites from Rundvågshetta, Lützow-Holm Bay, East Antarctica. The Antarctic Region: Geological Evolution and Processes, ed. by C.A. Ricci. Siena, Terra Antarct. Publ., 65–72.

Motoyoshi, Y. and Shiraishi, K. (1994): Quantitative chemical analyses of rocks with X-ray fluorescence analyzer (1) Major elements. Nankyoku Shiryô (Antarct. Rec.), **39**, 40–48 (in Japanese with English abstract).

Motoyoshi, Y., Matsubara, S. and Matsueda, H. (1989): *P-T* evolution of the granulite-facies rocks of the Lützow-Holm Bay region, East Antarctica. Evolution of Metamorphic Belts, ed. by J.S. Daly *et al.* Oxford, Geological Society (London), 325–329 (Geol. Soc. Spec. Publ. **43**).

Motoyoshi, Y., Thost, D.E. and Hensen, B.J. (1991): Reaction textures in calc-silicate granulties from the Bolingen Islands, Prydz Bay, East Antarctica: implications for the retrograde *P-T* path. J. Metamorph. Geol., **9**, 293–300.

Motoyoshi, Y., Hokada, T., Hiroi, Y. and Shiraishi, K. (2004): EMP dating on Cape Hinode of the Lützow-Holm Complex, East Antarctica. The 24th Symposium on Polar Geosciences, Program and Abstarcts, 14–15 October 2004. Tokyo, Natl Inst. Polar Res., 23.

Nakamura, Y. and Kushiro, I. (1970): Equilibrium relations of hypersthene, pigeonite and augite in crystallizing magmas: microprobe study of a pigeonite andesite from Weiselberg, Germany. Am. Mineral., **55**, 1999–2015.

Piazolo, S. and Markl, G. (1999): Humite- and scapolite-bearing assemblages in marbles and calc-silicates of Dronning Maud Land, Antarctica: new data for Gondwana reconstructions. J. Metamorph. Geol.,

17, 91–107.

Powell, R. and Holland, T.J.B. (2001): Course Notes for "THERMOCALC Workshop 2001: Calculating Metamorphic Phase Equilibria" (on CD-ROM).

Satish-Kumar, M. and Harley, S. L. (1998): Reaction textures in scapolite–wollastonite–grossular calc-silicate rock from the Kerala Khondalite Belt, Southern India: evidence for high-temperature metamorphism and initial cooling. Lithos, **44**, 83–99

Satish-Kumar, M. and Wada, H. (1997): Meteoric water infiltration in Skallen Marbles, East Antarctica: Oxygen Isotopic evidence. Proc. NIPR Symp. Antarct. Geosci., **10**, 111–119.

Satish-Kumar, M. and Wada, H. (2000): Carbon isotopic equilibrium between calcite and graphite in Skallen Marbles, East Antarctica: Evidence for preservation of peak metamorphic temperatures. Chem. Geol., **166**, 172–183.

Satish-Kumar, M., Yoshida, M., Wada, H., Niitsuma, N. and Santosh, M. (1998): Fluid flow along microfractures in calcite from a marble from East Antarctica: Evidence from gigantic (21‰) oxygen isotopic zonation. Geology, **26**, 251–254.

Satish-Kumar, M., Wada, H., Santosh, M. and Yoshida, M. (2001): Fluid-rock history of granulite facies humite-marbles from Ambasamudram, southern India. J. Metamorph. Geol., **19**, 395–410.

Satish-Kumar, M., Miyamoto, T. and Osanai, T. (2003): Causes for anomalous oxygen and strontium isotope compositions of marbles from Skallen, East Antarctica. Geochim. Cosmochim. Acta, **67**, A414.

Satish-Kumar, M., Tsunogae, T. and Osanai, Y. (2005): Development of fluid induced reactions, fracturing and compositional zoning in scapolite, Skallen, East Antarctica. J. Geol. Soc. Jpn., **111**, IX-X.

Satish-Kumar, M., Hermann, J., Tsunogae, T. and Osanai, Y. (2006a): Carbonation of Cl-rich scapolite boudins in Skallen, East Antarctica: evidence for changing fluid condition in the continental crust. J. Metamorph. Geol., **24**, 241–261.

Satish-Kumar, M., Kagashima, S., Suda, Y. and Motoyoshi, Y. (2006b): Geology of Byôbu Rock and Gobanme Rock, Prince Olav Coast, East Antarctica. Polar Geosci., **19**, 1–36.

Sengupta, S. and Raith, M.M. (2002): Garnet composition as a petrogenetic indicator: An example from a marble–calc-silicate granulite interface at Kondapalle, Easterm Ghats Belt, India. Am. J. Sci., **302**, 686–726.

Shiraishi, K., Ellis, D.J., Hiroi, Y., Fanning, C.M., Motoyoshi, Y. and Nakai, Y. (1994): Cambrian orogenic belt in East Antarctica and Sri Lanka: Implications for Gondwana assembly. J. Geol., **102**, 47–65.

Shiraishi, K., Hokada, T., Fanning, C. M., Misawa, K. and Motoyoshi, Y. (2003): Timing of thermal events in eastern Dronning Maud Land, East Antarctica. Polar Geosci., **16**, 76–99.

Tsuchiya, N., Osanai, Y. and Wada, H. (1992): Carbon and oxygen isotope compositions of marbles from the Sør-Rondane Mountains, East Antarctica. Recent Progress in Antarctic Earth Science, ed. by Y. Yoshida *et al.* Tokyo, Terra Sci. Publ., 55–59.

Valley, J.W. and Essene, E.J. (1980): Calc-silicate reactions in Adirondack marbles: the role of fluids and solid solutions. Geol. Soc. Am. Bull., **91**, 720–815.

Warren, R.G., Hensen, B.J. and Ryburn, R.J. (1987): Wollastonite and scapolite in Precambrian calc-silicate granulites from Australia and Antarctica. J. Metamorph. Geol., **5**, 213–223.

Yanai, K., Kizaki, K., Shiraishi, K., Hiroi, Y. and Kanisawa, S. (1984): Geological map of Akarui Point and Nag-iwa Rock. Antarctic Geological Map Series, Sheet 20 (with explanatory text 6 p.). Tokyo, Natl Inst. Polar Res.

Yoshida, M. (1977): Geology of the Skallen region, Lützow-Holmbukta, East Antarctica. Mem. Natl Inst. Polar Res., Ser. C (Earth Sci.), **11**, 38 p.

Yoshimura, Y., Motoyoshi, Y. and Miyamoto, T. (2003): Sapphirine-garnet-orthopyroxene granulite from Rundvågshetta in the Lützow-Holm Complex, East Antarctica. The 23rd Symposium on Polar Geosciences, Program and Abstarcts, October 2003. Tokyo, Natl Inst. Polar Res., 74 (in Japanese).

Yoshimura, Y., Motoyoshi, Y., Miyamoto, T., Grew, E.S., Carson, C.J. and Dunkley, D.J. (2004): High-grade metamorphic rocks from Skallevikshalsen in the Lützow-Holm Complex, East Antarctica: Metamorphic conditions and possibility of partial melting. Polar Geosci., **17**, 57–88.